Coherent and chaotic properties of nuclear pairing

Alexander Volya, Vladimir Zelevinsky, and B. Alex Brown
Department of Physics and Astronomy and National Superconducting Cyclotron Laboratory, Michigan State University, East Lansing, Michigan 48824-1321

(Received 7 September 2001; published 29 April 2002)

The properties of the pairing interaction in the shell model framework are considered with the aid of an exact numerical solution utilizing the quasispin symmetry. We emphasize the features which are out of reach for the usual approximate techniques based on the BCS approach supplemented by the random phase approximation treatment of pair vibrations, especially in the region of weak pairing where the BCS plus random-phase-approximation theory fails. Chaotic aspects of the mixing generated by the pairing interaction are studied. The level repulsion and large information entropy of the eigenstates coexist with the absence of thermalization of single-particle motion. The full spectrum of pair vibration on average displays a spin dependence similar to that for a rigid rotor.

DOI: 10.1103/PhysRevC.65.054312 PACS number(s): 21.60.−n, 71.10.Li, 21.60.Cs, 21.10.Ma

I. INTRODUCTION

Many properties of atomic nuclei are essentially governed by pairing interactions. Here and below we use ''pairing'' to describe the part of the residual interaction which scatters the particles between the pairs of time-conjugate single-particle orbits. The isoscalar pairing, which may be important for $N \approx Z$ nuclei far from stability, will not be discussed here (at a single spherical j level such $T=0$ pairing would require pairs with $J=1$), although it can also be studied in a similar manner.

Pairing is often viewed as a simple, and most regular, part of the nuclear interaction. In a low-lying region of the spectrum it forms a pair condensate which strongly influences all nuclear properties [1,2]. According to the standard BCS description borrowed from the macroscopic theory of superconductivity, the excitation of the system breaks pairs, removing them from the interaction domain and blocking the scattering phase space for remaining pairs. Another, collective mode of excitation implies the redistribution of the pairs with no breaking. As a result, coherent pair vibrations of the condensate are possible. At some excitation energy (or temperature) there occurs a sharp second-order phase transition to a normal-heated Fermi liquid where the pairing effects are usually neglected, again in the spirit of the BCS theory of macroscopic superconductors. However, closer consideration of the problem for finite systems such as nuclei reveals that there exist nontrivial effects resulting from pairing that persist through the entire shell-model spectrum. In nuclei the mesoscopic nature of the system smoothes all transitional phenomena, resulting in a more gradual change of properties.

Another (usually ignored) aspect of the pairing problem is that, along with the very coherent nature of the ground state, pairing brings in a certain degree of incoherent mixing. Our goal below is to study the pairing problem in full in order to present a consistent picture of the physical effects associated with the pairing interaction. For a broad range of energies we study the thermodynamical properties, entropy, thermalization, and mixing of simple configurations as well as coherent pair excitations, and average moments of inertia. A thorough consideration of pairing should precede the detailed study of the interplay of the pairing with other components of the residual interaction (a shell model analysis revealed [3] unexpected results of this interplay).

We study pairing in the framework of the realistic spherical nuclear shell model, which provides a perfect testing ground for discussing the phenomena of interest. There exist a number of approximate methods for curing the well-known shortcomings of the BCS approach for finite systems. However, they cannot be used for our purpose. Pairing fluctuations extending far below the BCS phase transition cannot be treated with the usual approximate techniques. The spectrum of excited states, including those at high energy, is also out of the reach of the most of approximations. Keeping this situation in mind, we consider the properties of the exact solution of a nuclear many-body problem with the pairing interaction [4], using an algorithm based on the quasispin method [5]. Earlier we showed [4] that such an exact numerical solution is convenient, is practically simple, and can be combined with new approaches for taking into account other parts of the residual interaction.

II. MODEL

We consider a general description of a finite Fermi system in the framework of the spherical shell model. Our space includes a set of j levels (of capacity $\Omega_j=2j+1$) with single-particle energies ϵ_j. The method [5,4] used here for solving the pairing problem is based exactly on the quasispin algebras present in the pairing Hamiltonian

$$H=\sum_j \epsilon_j N_j+\sum_{j,j'} \mathcal{V}_{jj'} P_j^\dagger P_{j'}. \tag{1}$$

Here $P_j^\dagger$ and P_j are pair creation and annihilation operators of particles on a j level,

$$P_j=\frac{1}{2}\sum_m \tilde{a}_{jm} a_{jm}, \quad P_j^\dagger=(P_j)^\dagger=\frac{1}{2}\sum_m a_{jm}^\dagger \tilde{a}_{jm}^\dagger, \tag{2}$$

where the tilde refers to time-conjugate states $\tilde{a}_{jm} \equiv (-)^{j-m} a_{j-m}$, and $\tilde{\tilde{a}}_{jm} = -a_{jm}$. The particle number operator in a given j level is $N_j = \Sigma_m a^\dagger_{jm} a_{jm}$.

Three operators

$$\mathcal{L}^-_j \equiv P_j, \quad \mathcal{L}^+_j \equiv P^\dagger_j, \quad \mathcal{L}^z_j \equiv \frac{1}{2}\left(N_j - \frac{\Omega_j}{2}\right) \tag{3}$$

close a quasispin SU(2) algebra; the corresponding classification of the basis is very useful in practical calculations. The quasispin formalism used here reduces the pairing problem to the problem of coupling of partial quasispins $\vec{\mathcal{L}}_j$ for individual j levels. We use a coupling scheme where the basis states are labeled with the absolute value $\mathcal{L}_j$ of the partial quasispin, or, alternatively, partial seniority $s_j = \Omega_j/2 - 2\mathcal{L}_j$, and particle number N_j for each single-particle level j related to the quasispin projection $\mathcal{L}^z_j$. In contrast to the occupancies N_j, all partial seniorities s_j are conserved by the pairing Hamiltonian as well as the full seniority of the system $s = \Sigma_j s_j$. The decomposition of the space into blocks labeled by the seniority quantum numbers simplifies the problem immensely. Although here we consider only one kind of particles, the technique can be extended for full isovector pairing [6–8].

As a realistic example we consider the shell-model description of the ^{116}Sn isotope. The valence neutron pairing is well known to play an important role in tin isotopes [9,10]. The model space consists of five single-neutron orbitals $h_{11/2}, d_{3/2}, s_{1/2}, g_{7/2}$, and $d_{5/2}$ with corresponding single-particle energies -9.76, -8.98, -7.33, -7.66, and -7.57 MeV. There are 601 080 390 many-body states, among those 272 828 have spin zero and can be partitioned into 420 different seniority sets. The dimension of the fully paired set of seniority zero (all $s_j = 0$) is 110.

In our analysis of the properties of pure pairing we set to zero all nonpairing parts of the effective interaction, and use the pairing matrix elements ($L = 0$ and $T = 1$) from the G matrix derived from the nucleon-nucleon interaction [11], with ^{132}Sn taken as a closed shell [12]. In this derivation the $\hat{Q}$-box method includes all nonfolded diagrams up to third order in the interaction and sums up the folded diagrams to infinite order [13]. In this way our input quantities in Hamiltonian (1) are completely determined. Calculations with these parameters, using direct shell-model diagonalization, as well as the exact pairing (EP) plus monopole technique [4], are in a good agreement with experimental data [14]. We need to stress, however, that our main results and the general discussion are insensitive to the precise choice of the pairing matrix elements.

III. PAIR VIBRATIONS AND COMPLEXITY OF EIGENSTATES

The pairing interaction of Eq. (1) contains the elementary processes of pair transfer from one single-particle orbital to another. Since the pairs are not broken, the interaction is only capable of mixing the independent-particle configurations within the same seniority set $\{s_j\}$. We refer to the amplitude of such a process as that of a pair vibration. Pair vibrations were first proposed by Bohr [15] addressing the collective nature of low-lying 0^+ states. A number of other studies followed [16] with a discussion of the collective excitations of the pair condensate in the BCS plus random-phase-approximation (RPA) framework. The weakening of the static pairing near the subshell closure of ^{114}Sn implies strong fluctuations and mixing of configurations in this region that may effect the quality of BCS-based theories in the description of the observed states in Sn nuclei.

As we mentioned, the total number of the states $J^\pi = 0^+$ in the valence space of ^{116}Sn that have no broken pairs (total seniority $s = \Sigma_j s_j = 0$) is equal to 110. The ground state corresponds to the BCS-like coherent alignment of quasispins in the condensate which produces minimum energy and average occupancies N_j which in the BCS limit would be determined by the Bogoliubov transformation coefficients $v^2_j = \overline{N_j}$ and $u^2_j = 1 - \overline{N_j}$. The pair scattering between the shell model basis configurations is responsible for their complicated mixing. In what follows we first analyze the degree of complexity of the resulting eigenstates with the aid of information (Shannon) entropy and invariant correlational (von Neumann) entropy [17,18,3] and then try to single out the collective pair vibration modes, comparing them with the RPA.

The information entropy I_α of the eigenstates $|\alpha\rangle$ with respect to the basis $|k\rangle$ was repeatedly used for characterizing the degree of mixing and delocalization of the eigenfunctions expressed in the original ''unperturbed'' basis [17,19–22]. As discussed in [3,23], the annoying basis dependence of this quantity may be advantageous in providing additional knowledge about the dynamic interrelation between the reference basis and the eigenbasis of the Hamiltonian. For example, it was shown recently [24] that for a shell-model system with *random* two-body interactions, the information entropy of the eigenstates expressed in the basis of the stationary states generated by the realistic effective interaction does not evolve along the spectrum, being steadily close to the random matrix theory limit. This means that the wavefunctions of a system with random interactions are delocalized all over the spectrum of the realistic eigenstates. Contrary to this, in the mean-field (shell-model) basis both sets of eigenstates display the regular energy dependence typical for the strong mixing at high level density.

In Fig. 1, the information entropy of all 110 states with $s = 0$ is shown as a function of state energy E_α. The information entropy of an eigenstate $|\alpha\rangle$,

$$I_\alpha = -\sum_k |C^\alpha_k|^2 \ln(|C^\alpha_k|^2), \tag{4}$$

is defined through its decomposition in terms of the basis components $|k\rangle$:

$$|\alpha\rangle = \sum_\alpha C^\alpha_k |k\rangle. \tag{5}$$

Each basis state $|k\rangle$ corresponds to a distribution of particle pairs over single-particle levels in such a way that each level

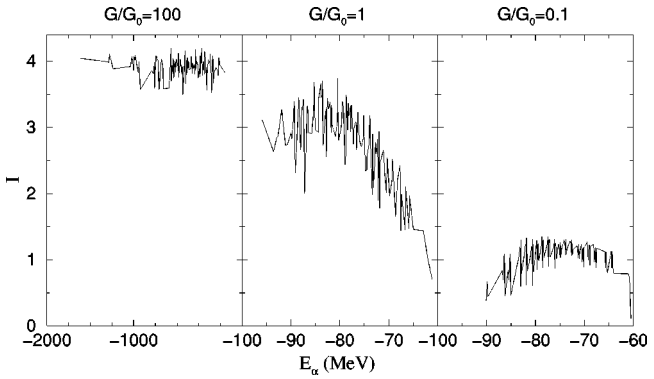

FIG. 1. Information entropy of seniority zero states in ^{116}Sn plotted vs their energy. The middle panel corresponds to the realistic values of the pairing matrix elements, for the left panel the pairing is enhanced by a factor of 100, and for the right panel the pairing is reduced by a factor of 10.

has an even number of particles and they are all paired. The basis wave functions for 110 different pairwise rearrangements of 16 valence neutrons in the ^{116}Sn shell-model space are explicitly built by the action of the operators $(P_j^\dagger)^{N_j}$, and correctly normalized taking into account the blocking effects.

Three panels in Fig. 1 show the entropy I_α as a function of energy E_α for various pairing strengths measured with the aid of the overall scaling factor G/G_0 in pair transfer-matrix elements. The results are not symmetric with respect to the centroid of the spectrum, since the states of $s=0$ comprise only a part of all states with spin $J=0$; the remaining states have seniority 4 and higher. Average information entropy of states in the extreme limit of randomness given by the Gaussian orthogonal ensemble (GOE) is predicted to be [21,25,3]

$$I_{\mathrm{GOE}} = \ln(0.482\mathcal{N}), \tag{6}$$

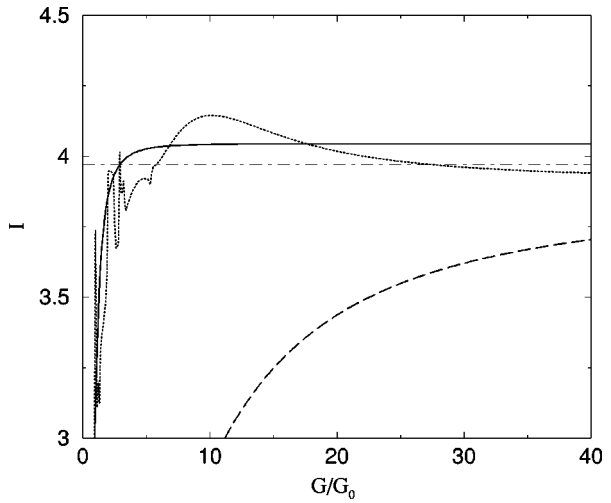

FIG. 2. Information entropy of selected seniority zero states in ^{116}Sn as a function of the pairing strength. The chosen states are the ground state (solid line), the 50th state (in order by energy, dotted line) and the highest, 110th, state (dashed line).

where $\mathcal{N}$ is the space dimension. In our case of $\mathcal{N}=110$, the GOE limit would give $I_{\mathrm{GOE}}=3.97$. As seen from Fig. 1, the complexity of states increases with the pairing strength and reaches the GOE limit for strong pairing. Already the realistic pairing strength provides a strong mixing of all states with some reduction toward the ends of the spectrum. The asymmetry of I_α as a function of E_α is related to the asymmetry of the single-particle energies in the shell. The highest states mainly correspond to the occupation of the highest orbits (''negative temperature''). Because of the relatively large energy gap between these levels and the remaining (lowest) unoccupied ones $h_{11/2}$ and $d_{3/2}$, the pairing interaction is less effective in state mixing.

Being a measure of the delocalization of the eigenstates in an unperturbed basis, information entropy cannot distinguish between a coherent superposition of simple excitations characteristic of collective modes and a chaotic combination which emerged from complicated incoherent dynamics [3]. (The distinction would require different tools, such as invariant correlational entropy [18]; see the discussion of Fig. 3 below.) Figure 2 demonstrates the behavior of information entropy at large pairing strengths. The highest excited state approaches the GOE limit very slowly since, being formed as the ''antipaired'' combination at weak pairing, it is already shifted up in the second order of perturbation theory so that further mixing becomes suppressed. A similar effect of the shift down exists for the ground state as well, but here the collectivity significantly increases the value of the entropy. The ground-state entropy is saturated even above the GOE limit, indicated in the figure by a thin solid line. For very strong pairing single-particle energies can be neglected, turning the problem into the degenerate model case for $\mathcal{V}_{jj'}$ = const; the realistic interaction is close to this limit. In terms of quasispin, different recoupling schemes can be used to construct the basis [5]. The basis states used in EP are labeled both by the partial quasispins and their projections appropriate for the weak coupling limit with the distribution of particles close to the Fermi step function. The basis of total quasispin and different recoupling quantum numbers may serve better in the strong pairing (degenerate) limit. In terms of the particle distribution, the strong pairing limit with $\mathcal{V}_{jj'}=$ const results in the equipopulation of the sublevels (''infinite temperature'').

At low pairing strengths (the case of $G/G_0=0.1$ in Fig. 1), the quality of the occupation number basis is improved due to the increased role of the mean-field energies. Here the BCS theory would show no condensate formation, since the spacings between the single-particle levels are greater than the pairing strength by an order of magnitude. However, in the exact solution, the pair fluctuations still provide a considerable mixing that persists throughout the spectrum.

IV. RANDOM PHASE APPROXIMATION IN THE QUASISPIN FORMALISM

A. RPA equations

Our exact solution obtained by a direct diagonalization in the small space of seniority $s=0$ can be compared with the standard BCS solution supplemented by the random phase

approximation for the collective modes related to pair vibrations. We start with formulating the BCS+RPA approach in the quasispin formalism. For macroscopic superconductors (with all partial spins equal to $j=1/2$), such an approach was used in the classic paper by Anderson [26]. Since the particle number in this approach is assumed to be preserved only on average, one needs to introduce the chemical potential μ.

The pairing field can be written as a linear functional of one of the quasispin operators $\mathcal{L}$:

$$\Delta_j\{\mathcal{L}\}=\sum_{j'}\mathcal{V}_{jj'}\mathcal{L}_{j'}. \tag{7}$$

The operator equations of motion for the partial quasispin components with the pairing Hamiltonian are

$$[\mathcal{L}_j^x,H]=-2i\epsilon_j'\mathcal{L}_j^y+i[\mathcal{L}_j^z,\Delta_j\{\mathcal{L}_j^y\}]_+, \tag{8}$$

$$[\mathcal{L}_j^y,H]=2i\epsilon_j'\mathcal{L}_j^x-i[\mathcal{L}_j^z,\Delta_j\{\mathcal{L}_j^x\}]_+, \tag{9}$$

$$[\mathcal{L}_j^z,H]=i[\mathcal{L}_j^y,\Delta_j\{\mathcal{L}_j^x\}]_+-i[\mathcal{L}_j^x,\Delta_j\{\mathcal{L}_j^y\}]_+, \tag{10}$$

where $[A,B]_+\equiv AB+BA$ denotes the anticommutator, and we introduced the corrected single-particle energies $\epsilon_j'=\epsilon_j+\mathcal{V}_{jj}/2-\mu$.

The BCS solution corresponds to the static mean-field alignment of partial quasispins; the spread of the single-particle energies plays the role of the magnetic field along the z axis. The direction of alignment in the xy plane is chosen arbitrarily (spontaneous symmetry breaking); for instance, we take it in such a way that $\langle\mathcal{L}_j^y\rangle=0$. The static solution can be derived from the diagonal matrix elements of the equations of motion. We denote the static amplitudes of $\mathcal{L}_j^z$ and $\mathcal{L}_j^x$ as Z_j and X_j, respectively. Linearizing the equations of motion for off-diagonal matrix elements, we obtain normal modes of pair vibrations in the harmonic approximation. It is convenient to introduce collective coordinates α and corresponding conjugate momenta π and look for a solution of the form

$$\mathcal{L}_j^x=X_j+x_j\alpha+\cdots,\quad \mathcal{L}_j^y=y_j\pi+\cdots,$$
$$\mathcal{L}_j^z=Z_j+z_j\alpha+\cdots \tag{11}$$

(in the harmonic approximation the distinction between the coordinates and momenta is a matter of convention). Searching for the excitation in a given nucleus, we need to impose the average particle number conservation condition. With definition (3) of the operator $\mathcal{L}_j^z$, the total particle number operator is

$$N=\sum_j\left(\frac{\Omega_j}{2}+2\mathcal{L}_j^z\right)\equiv\frac{\Omega}{2}+2\mathcal{L}^z. \tag{12}$$

In operator expansion (11) this means that the static and oscillating amplitudes of $\mathcal{L}_j^z$ should satisfy

$$N=\frac{\Omega}{2}+2\sum_j Z_j,\quad \sum_j z_j=0. \tag{13}$$

The BCS equation for the static part is to be found from the expectation value of the right hand side of the y-equation (9),

$$X_j=\frac{\Delta_j\{X\}}{\epsilon_j'}Z_j. \tag{14}$$

The normalization of the static amplitudes comes from the condition for the maximum value of the total quasispin in the ground state:

$$X_j^2+Z_j^2=\vec{\mathcal{L}}_j^{\,2}=\frac{\Omega_j}{4}\left(\frac{\Omega_j}{4}+1\right)\approx\left(\frac{\Omega_j}{4}\right)^2. \tag{15}$$

The solution can now be written in the forms

$$X_j=-\frac{\Omega_j}{4e_j}\Delta_j\{X\},\quad Z_j=-\frac{\Omega_j}{4e_j}\epsilon_j', \tag{16}$$

where the quasiparticle energies are $e_j=+\sqrt{\epsilon_j'^2+\Delta_j^2\{X\}}$, and the gap equation for $\Delta_j\equiv\Delta_j\{X\}$ is the same as in the BCS theory:

$$\Delta_j=-\sum_{j'}\mathcal{V}_{jj'}\Omega_{j'}\frac{\Delta_{j'}}{4e_{j'}}. \tag{17}$$

The first condition (13) of particle number conservation determines the chemical potential in full agreement with the BCS where the occupation factors are $v_j^2=(1/2)[1-(\epsilon_j'/e_j)]$.

Using the harmonic oscillator collective Hamiltonian $H=(\pi^2+\omega^2\alpha^2)/2$ with frequency ω, for the RPA amplitudes x_j,y_j, and z_j, defined in Eq. (11), we obtain

$$\omega^2x_j=-2\epsilon_j'y_j+2Z_j\Delta_j\{y\}, \tag{18}$$

$$-y_j=2\epsilon_j'x_j-2Z_j\Delta_j\{x\}-2\Delta_jz_j, \tag{19}$$

$$\omega^2z_j=2\Delta_jy_j-2X_j\Delta_j\{y\}. \tag{20}$$

The spurious mode of this set, $\omega=0$, gives, either from Eq. (18) or from Eq. (20), the solution for y_j coinciding with that for the static amplitude X_j [Eq. (16)]. This obviously corresponds to the Goldstone rotation of the condensate phase. The spurious mode related to the change of the particle number is generated by the operator $\alpha\Sigma_jz_j$; see the second condition in Eq. (13). However it does not contribute to physical modes, since the sum over j in Eq. (20) identically vanishes due to the symmetry of the kernel $\mathcal{V}_{jj'}$. Looking for nonspurious solutions with $\omega\neq0$ and eliminating the coordinate amplitudes x_j and z_j, we come to the equation for the momentum amplitude y_j which determines the physical normal modes,

$$(4e_j^2-\omega^2)y_j=-e_j\Omega_j\Delta_j\{y\}+2Z_j\Delta_j\{t\}, \tag{21}$$

where the last term contains the same functional Δ [Eq. (7)], taken for

$$t_j = \epsilon'_j \left(2y_j + \frac{\Omega_j}{2e_j} \Delta_j \{y\} \right). \tag{22}$$

This secular equation is also valid for the normal modes generated by pairing with no condensate present when we have only the trivial BCS solutions $X_j = 0$ and $\Delta_j = 0$, the vibrational amplitude z_j vanishes, and the single-particle energies are equal to $|\epsilon'_j|$. With the extension to higher orders of the same mapping procedure to the collective variables as in Eq. (11), one can study the anharmonic effects. However, if the anharmonicity is indeed important, as for example in the region of very low frequencies and correspondingly large amplitude collective motion, it is simpler (at least in the pure pairing problem) to switch to the exact solution.

B. Example: two-level system with off-diagonal pairing

As an example of the analytically solved RPA, we consider an interesting particular case of two levels with capacities $\Omega_{1,2}$ and single-particle energies $\epsilon_{1,2}$ when the pairing interaction has only the off-diagonal amplitude $\mathcal{V}_{12} = \mathcal{V}_{21} \equiv g$ (in this case the sign of g does not matter). With the effective interaction parameters $\lambda_{1,2} = g\Omega_{1,2}/4$, the set of the BCS gap equations (17) takes the forms

$$\Delta_1 = \frac{\lambda_2}{e_2} \Delta_2, \quad \Delta_2 = \frac{\lambda_1}{e_1} \Delta_1, \tag{23}$$

which leads to the exact solutions

$$\Delta_1^2 = \frac{\lambda_1^2 \lambda_2^2 - \epsilon_1'^2 \epsilon_2'^2}{\lambda_1^2 + \epsilon_2'^2}, \quad \Delta_2^2 = \frac{\lambda_1^2 \lambda_2^2 - \epsilon_1'^2 \epsilon_2'^2}{\lambda_2^2 + \epsilon_1'^2}. \tag{24}$$

The corresponding quasiparticle energies are given by

$$e_1^2 = \lambda_1^2 \frac{\lambda_2^2 + \epsilon_1'^2}{\lambda_1^2 + \epsilon_2'^2}, \quad e_2^2 = \lambda_2^2 \frac{\lambda_1^2 + \epsilon_2'^2}{\lambda_2^2 + \epsilon_1'^2}, \tag{25}$$

with the useful identity

$$e_1 e_2 = \lambda_1 \lambda_2 \tag{26}$$

being valid. The BCS solution collapses, $\Delta_{1,2} \to 0$, at the critical coupling strength determined by $\lambda_1^2 \lambda_2^2 = \epsilon_1'^2 \epsilon_2'^2$, or at

$$g^2 \to g_c^2 = \frac{16 |\epsilon'_1 \epsilon'_2|}{\Omega_1 \Omega_2}. \tag{27}$$

The secular equation [see Eqs. (21) and (23)], with the help of identity (26), gives, along with the spurious mode $\omega^2 = 0$, the physical root

$$\omega^2 = 4(e_1^2 + e_2^2 + 2\epsilon'_1 \epsilon'_2) = 4[(\epsilon'_1 + \epsilon'_2)^2 + \Delta_1^2 + \Delta_2^2]. \tag{28}$$

C. Exact solution versus BCS+RPA

The behavior of energies and entropy in the BCS phase transition region is illustrated in Fig. 3 for a two-level model, and in Fig. 4 for the realistic case. First we consider the two-level model, defined in Sec. IV B; see Fig. 3. In the case of half occupancy and two levels of equal capacity, $N = \Omega_1 = \Omega_2$, with energies $\pm\epsilon$ symmetric with respect to the chemical potential $\mu = 0$, the RPA predicts $\omega^2 = 8\Delta^2$, see Eq. (28). Note that in the case of many interacting levels with $\mathcal{V}_{jj'} = \text{const}$ the spectrum of normal modes starts with the lower value $\omega^2 = 4\Delta^2$ (the threshold of pair breaking).

Panel (b) in the middle shows the energies of the lowest pair vibration state (thick solid line) and the lowest state with one broken pair (thick dashed line) as a function of the pairing strength g. The excitation energy of the pair vibration is compared with the RPA prediction shown by the thin dotted line. The BCS phase transition occurs, in the units corresponding to $|\epsilon_{1,2}| = 1$, at $g = g_c = 0.25$, where we see the breakdown of the RPA and the vanishing collective frequency. Below this point the RPA is constructed on the background of the normal Fermi distribution, while, above $g = g_c$ the RPA is built on the pairing condensate. The limits $g \to 0$ and $g \to \infty$ are described well within the RPA, while near the phase transition large fluctuations make the BCS +RPA description unreliable. The failure of the BCS is well discussed in the literature and studied using simple models [27]. In accordance with this instability, a sharp rise of en-

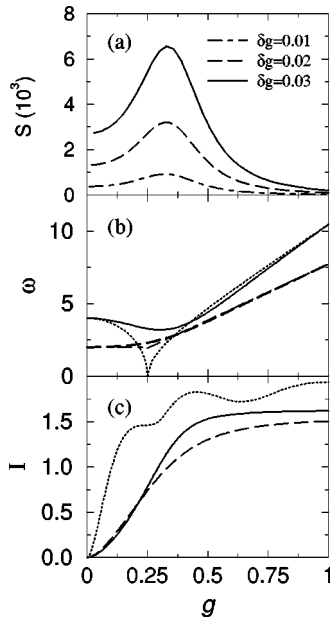

FIG. 3. Two-level pairing model $N = \Omega_1 = \Omega_2 = 16$; only the off-diagonal pair transfer amplitude $\mathcal{V}_{12} = \mathcal{V}_{21} = g$ is taken into account. The upper plot (a) displays the invariant entropy (see the text), of the ground state for $\delta g = 0.01$, 0.02, and 0.03 averaging intervals. The middle part (b) shows the excitation energy of the lowest pair vibration state (thick solid line). The thin dotted line approximates this curve with the aid of the RPA built on the normal Fermi ground state on the left of the phase transition point at $g = 0.25$ and on the BCS ground state on the right of the critical point. The thick dashed line shows the excitation energy of the lowest state with broken pair $s = 2$. This curve is compared with $2e$ (thin dot-dashed curve), the BCS energy of a two-quasiparticle state. The lower panel (c) displays information entropy for the ground state (solid line), second pair vibration excited state $s = 0$ (dotted line), and the lowest $s = 2$ state (dashed line).

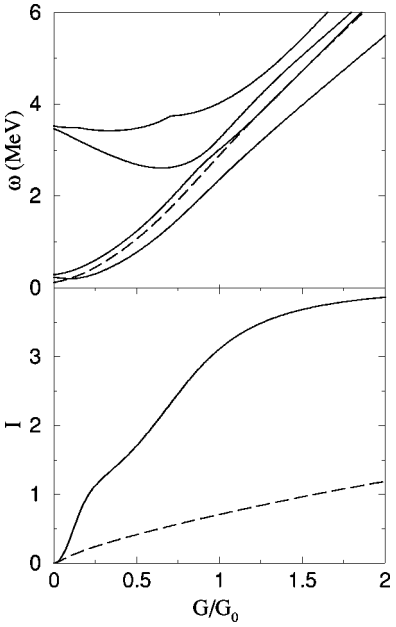

FIG. 4. Upper panel: excitation energies of low-lying states in the shell model for ^{116}Sn as a function of relative pairing strength G/G_0, the lowest pair vibration states with $s=0$ (solid line) and the lowest $s=2$ state (dashed line). Lower panel: information entropy of the ground state (solid line) and and the most excited paired state $s=0$ (dashed line).

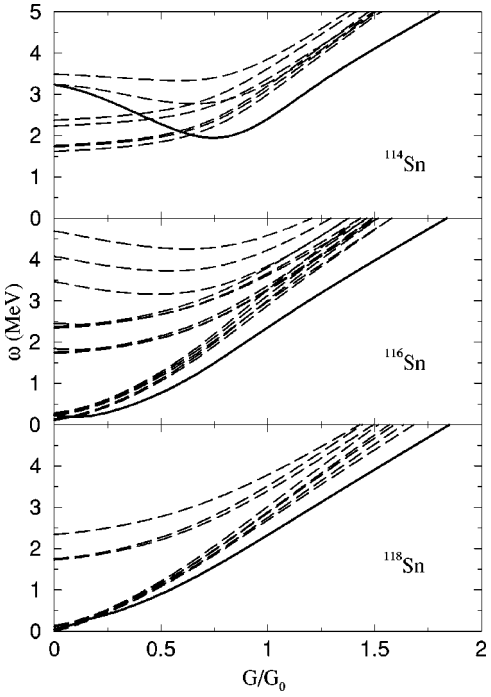

FIG. 5. Excitation energies of low-lying $s=2$ states (dashed lines) are compared with that of the lowest pair-vibration state $s=0$ shown (solid line) as a function of the relative pairing strength. The three panels correspond to ^{114}Sn, ^{116}Sn, and ^{118}Sn isotopes.

tropy takes place in the vicinity of $g=g_c$ showing a dramatic restructuring of the eigenstates when the independent pair basis states become strongly mixed. One needs to emphasize here that, even for a very strong interaction, the limit of the degenerate seniority model is never reached if the pair transfer matrix elements are different for different pairs, in contrast to the model with constant pairing when all $\mathcal{V}_{jj'}=g=$const.

Figure 3(b) addresses the question of the nature of the first excited state. The breaking of a pair requires a two-quasiparticle excitation energy of $2e$ that is plotted with a thin dashed line, which has in the asymptotic limit of strong pairing the value of twice the BCS gap. In realistic nuclear systems unpaired particles may still interact attractively, therefore reducing this energy even further. The lowering of a two-quasiparticle quadrupole mode is especially strong in the case of collective vibrations near the onset of deformation. The lowest state of pair vibrations, which has zero spin, is usually much higher in energy. It is possible in principle that the state of pair vibrations becomes the lowest excited state. For example, this can be the case when two single-particle orbitals lie very close in energy making a pair transfer energetically more favorable then breaking a pair. This feature is not present in the two-level model and the lowest thick dashed line, corresponding to the $s=2$ state in the plot in Fig. 3(b), is always lower than the thick solid line representing the pair vibrations.

In the ^{116}Sn model, the upper plot of Fig. 4, the lowest excited 0^+ state is of a pair-vibration nature. This pattern persists through the entire range of couplings displayed. The same trend is observed in other Sn isotopes (Fig. 5) including the case of ^{114}Sn with G/G_0 above 0.7. Here subshell closure requires a higher energy for the $s=0$ pair vibration which in the limit of weak pairing is just a two-particle-two-hole excitation of the normal Fermi ground state. It comes from the fact that there exist close single-particle levels that are not fully occupied and thus opened for low-energy pair vibrations. In ^{116}Sn these are the $h_{11/2}, d_{3/2}$, and $s_{1/2}$ levels, which are separated by only a few hundred keV. Because of the presence of other interactions, this prediction for the first excited state is not fulfilled in reality. Still, a number of low-lying 0^+ states is observed in Sn isotopes. The nature of these states is complex, being influenced by other phenomena such as proton core excitation and shape coexistence [28]. Moreover, the effect of other interactions can be important through the admixture of seniority $s=4$ states that may have collective structure of a two-phonon excitation. In Fig. 6 excitation energies of the two lowest pair vibration states are compared with the experimentally observed states that are expected to be mostly of a pair vibration nature; see Ref. [28] and references therein. The agreement is satisfactory considering the crudeness of the pure pairing model and the uncertainties in the pair transfer strengths and single-particle energies.

It was already discussed in the literature that even though pairing is generally quite strong in Sn isotopes there is some weakening in the region of ^{114}Sn due to the nearly 2-MeV shell gap between the $h_{11/2}, d_{3/2}$, and $s_{1/2}$ levels and the rest of the single-particle orbitals [4]. The proximity of the BCS phase transition results in a rapid growth of information entropy in this region, see Fig. 4, lower panel. This also leads to a large excitation energy of the lowest pair-vibration state

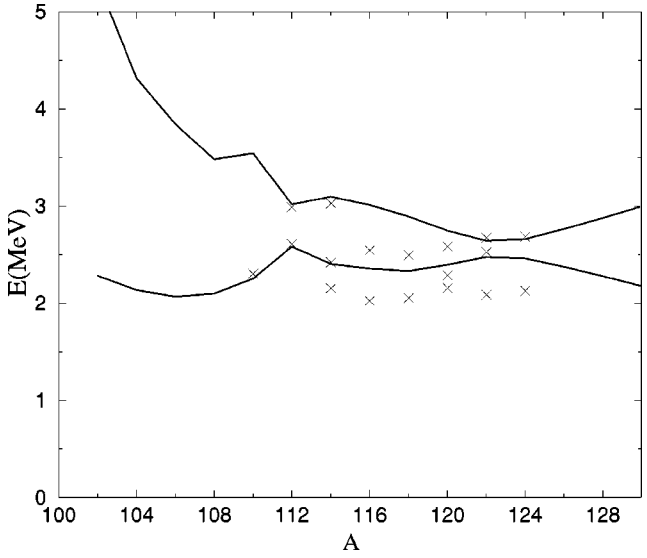

FIG. 6. Excitation energies of the lowest two-pair vibration states are plotted as a function of the nuclear mass A for Sn isotopes. Experimentally measured energies of the lowest spin-0 states, that are expected to have strong $s=0$ components, are shown for comparison.

in ^{114}Sn at relatively weak pairing (Fig. 5). The large configuration mixing in the region of a subshell closure is supported by experimental observations in the two-neutron pickup reaction [29] and has a direct manifestation in the increase of information entropy.

The randomizing aspect of pair vibrations is somewhat limited to the region near the BCS phase transition, where many recoupling schemes of quasispin become equiprobable. A similar phenomenon for angular momentum is known as geometric chaoticity [30] where the many-particle states of good total spin constructed by various recoupling schemes have an equivalent mixing (entropy). With no preference for any particular way of coupling, a minor change in the interaction may lead to a complete restructuring of the spectrum, a phenomenon similar to chaoticity. To emphasize the appearance of chaoticity in the BCS phase-transition region, the invariant entropy for a two-level model is presented in Fig. 3(a). The invariant entropy (basis independent) shows the degree of restructuring that happens in the eigenstate in response to a change δg in the interaction parameter g. The invariant (von Neumann) entropy of an eigenstate $|\alpha\rangle$ is determined with the aid of the density matrix ρ^{α},

$$S_{\alpha} = -\mathrm{Tr}\{\rho^{\alpha} \ln \rho^{\alpha}\}, \tag{29}$$

which is defined as an average over a region of parameters

$$\rho^{\alpha}_{kk'}(g,\delta g) = \frac{1}{\delta g}\int_{g}^{g+\delta g} C^{\alpha}_{k'} {}^{*} C^{\alpha}_{k}. \tag{30}$$

The invariant entropy in Fig. 3(a) is peaked in the phase-transition region, indicating a very sensitive (chaotic) dependence of an eigenstate on the interaction strength. Similar sharp enhancements of invariant entropy near the phase transitions were found in interacting boson models [31].

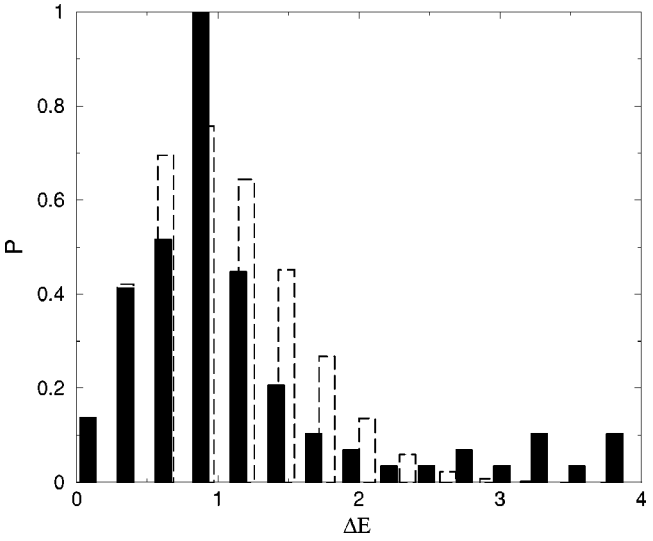

FIG. 7. The nearest-neighbor spacing distribution of $s=0$ states in ^{116}Sn (filled histogram) and the GOE distribution (open columns).

V. LOCAL SPECTRAL STATISTICS

The nearest-neighbor spacing distribution P shown in Fig. 7 is very close to that of the GOE exhibiting the features of level repulsion. However, the tail of the distribution is not Gaussian; it reveals an enhanced fraction of large gaps between the levels.

The so-called spectral rigidity, or Δ_3 statistics, is the more sensitive probe of spectral chaoticity. Figure 8 indicates a pseudorandom character of the spectra of the exactly solved pairing problem. The spectral rigidity is given as a function of L, the length of the fitted interval, whereas averaging over all starting points of such (overlapping) intervals is assumed. In Fig. 8 the spectral rigidity of paired states in ^{116}Sn is compared with the chaotic (GOE) distribution and regular Poisson-type behavior. The linear low-L behavior of the spectral rigidity is Poisson-like, while for larger intervals,

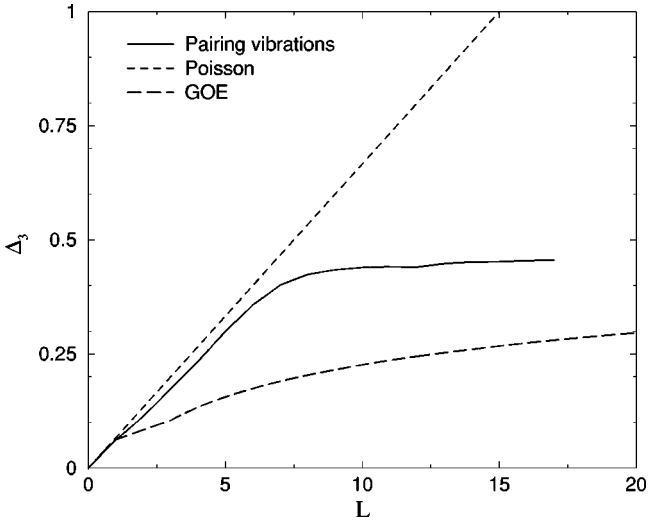

FIG. 8. The spectral rigidity (Δ_3 statistics) of paired states in ^{116}Sn compared to that of the GOE and Poisson distributions.

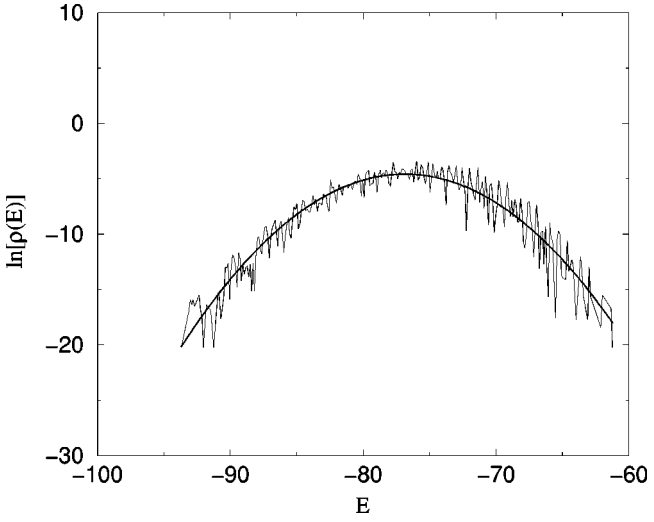

FIG. 9. Density of states in ^{116}Sn from the exact solution with the pairing interaction as a function of energy.

starting from around $L=7$, the regularities of the spectrum flatten the curve as an evidence of the oscillatory behavior associated with a regular quasiharmonic component in the spectrum. In fact, we are dealing here with the nonstandard situation of a local level repulsion supplemented by the presence of a vibrational order.

VI. PROPERTIES OF PAIRING THROUGH THE ENTIRE SPECTRUM

A. Level density

Even if the mixing is strong the amount of states with a given seniority is very limited. For the lowest seniority this number is small compared to the total number of states in the truncated Hilbert space. Globally the level repulsion (Fig. 7) is responsible for the widening of the entire spectrum. The density of states in the Hamiltonian systems governed by two-body interactions and described by finite matrices is generically close to Gaussian (the same is true for the limiting case of no residual interaction [32]). Pairing is very typical in this sense. Figure 9 shows the density of states in ^{116}Sn found from the exact solution of the pairing problem. The resulting curve is well fit by a Gaussian.

The parameters of the Gaussian are the lowest moments of the Hamiltonian which consists of single-particle and pairing parts:

$$H=H_{\rm sp}+\frac{G}{G_0}H_{\rm p}. \tag{31}$$

The centroid of the density distribution is given by the trace of the Hamiltonian,

$$\overline{H}=\frac{1}{\mathcal{N}}{\rm Tr}(H), \tag{32}$$

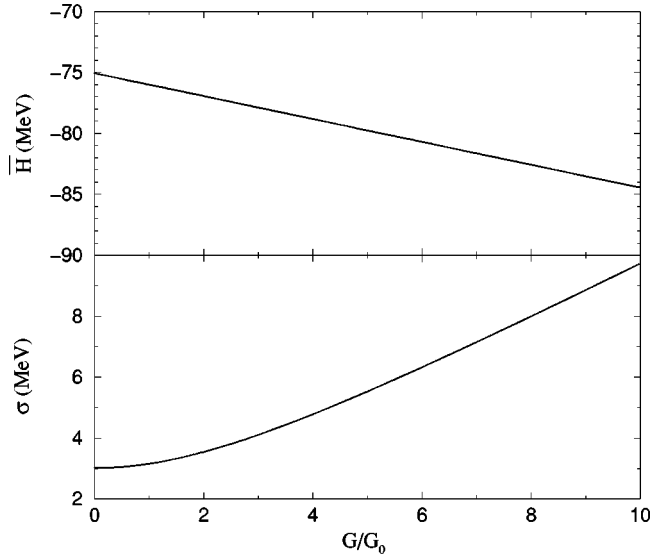

FIG. 10. The centroid (upper panel), and width of the density of states (lower panel) in the pairing model of ^{116}Sn as a function of the relative pairing strength. The empirical curve for the width is indistinguishable from the fit of Eq. (34).

where $\mathcal{N}$ is the total number of states (or levels for the case of $J=0$) in the shell-model space under consideration. The width of the level density is the mean square deviation of the Hamiltonian:

$$\sigma^2=\overline{H^2}-\overline{H}^2. \tag{33}$$

In general the dependence of the width on the coupling strength G/G_0 can contain a linear term as well as a quadratic term. As shown in the analysis of the statistical properties of the shell-model solutions [3], the two widths, a combinatorial one for noninteracting particles and a dynamical one due to the residual interaction, are added in quadratures. This is possible if the two parts of Hamiltonian (31) are statistically independent; $\overline{H_{\rm sp}H_p}=\overline{H_{\rm sp}}\,\overline{H_p}$.

In Fig. 10 the mean value and the width of the level density distribution are shown as functions of the relative pairing strength G/G_0. The location of the centroid of the level density is linear in the coupling strength, while the width is exactly fit by

$$\sigma=\sqrt{\sigma_{\rm sp}^2+\left(\frac{G}{G_0}\sigma_{\rm int}\right)^2}\ , \tag{34}$$

where the single-particle (non-interaction) width $\sigma_{\rm sp}=3.01$ MeV, and the pairing width $\sigma_{\rm int}=0.857$ MeV add in quadratures. In the region of the realistic strength the single-particle contribution to the width is by far the more dominant.

B. Pairing and thermalization

A closed mesoscopic system can in principle be analyzed solely in terms of individual eigenstates and energy eigenvalues. However, in the region of high level density, a statistical description operating with thermodynamical concepts is very

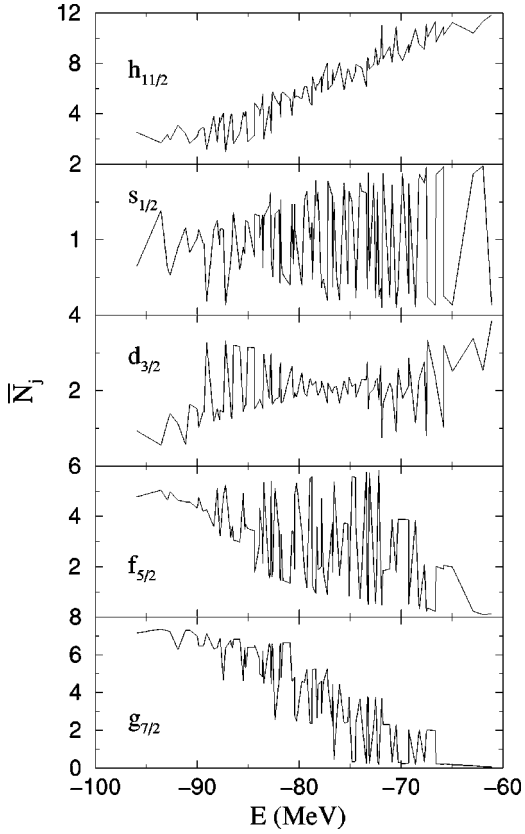

FIG. 11. Average occupancies of five single-particle orbitals for all 110 $s=0$ states in ^{116}Sn as a function of energy.

appealing. It was shown both for complex atoms and nuclei [33,3] that the increase of chaotic mixing with excitation energy and level density is in a sense equivalent to the process of thermalization, and can be treated with the help of a temperature. Moreover, the presence of such mixing is necessary in order to make the neighboring eigenstates ''look the same'' [34] and to justify the statistical averaging as in a microcanonical ensemble [3,23]. In particular, it turned out that the average occupation numbers of single-particle orbitals can be described by the Fermi-Dirac distribution even in the presence of strong interactions, although the single-particle energies can be renormalized to become those of quasiparticles. Thus, in the statistical region of the spectrum, we come effectively to the picture of a heated Fermi-liquid.

However, it is not clear that a specific interaction such as pairing can lead to full thermalization. As shown in Fig. 11, the occupancies of single-particle levels derived for the eigenstates of the pairing problem vary on average monotonously with energy, therefore showing a trend to thermalization. At the same time, there are wild fluctuations which would be even further enhanced if states of different seniorities were included.

To address the thermalization we can define various temperature scales [33,3]. The thermodynamical ''absolute temperature'' comes from the density of states

$$\frac{dS_\rho(E)}{dE}=\frac{1}{T_{\rm abs}}, \quad \text{where} \quad \rho(E)=e^{S_\rho(E)}; \tag{35}$$

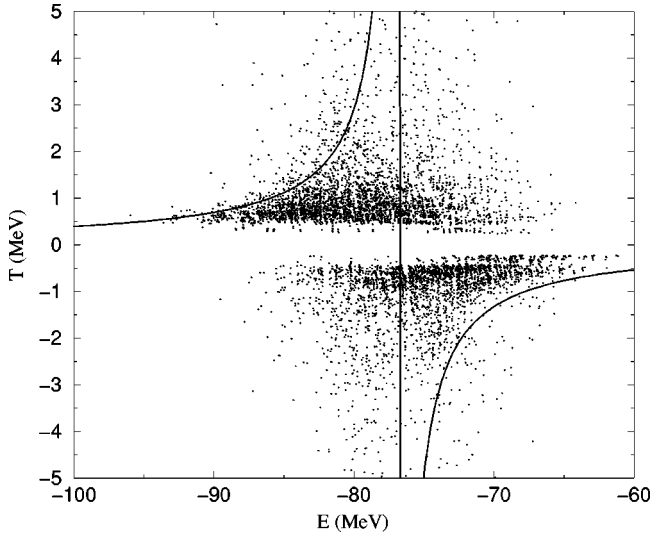

FIG. 12. Absence of spectral thermalization in ^{116}Sn from the comparison of absolute temperature [Eq. (35)] (solid line), with single-particle temperature that follows from the neutron distribution over single-particle orbitals Eq. (37).

therefore,

$$T_{\rm abs}(E)=\frac{\sigma^2}{\overline{H}-E}. \tag{36}$$

The ''single-particle'' temperature T_{s-p} is linked to the termalization of the system in terms of the distribution of particles over single-particle levels. It can be determined for each individual eigenstate from the best fit of the occupation numbers to the Fermi-Dirac distribution

$$\overline{N}_j=\frac{\Omega_j}{e^{(\epsilon_j-\mu)/T_{s-p}}+1}, \tag{37}$$

where the chemical potential μ also can be determined from the two-parameter fit.

In Fig. 12 the comparison of these two definitions of temperature for all states in ^{116}Sn is shown. The result is very different from what was observed in the shell model taking into account all residual interactions where $T_{\rm abs}$ and T_{s-p} were in a good agreement for the majority of eigenstates (a similar thermalization occurs as well when random residual interactions are taken). With the pairing interaction only, the dots representing T_{s-p} of individual eigenstates show a low temperature along the entire spectrum, whereas the smooth hyperbola corresponds to absolute temperature which has a singularity in the middle of the spectrum. It is clear that the single-particle thermometer cannot measure correctly the temperature of the paired system.

VII. ROTATION OF A PAIRED SYSTEM

A pure pairing fermionic condensate has properties similar to those observed in macroscopic superfluid systems. Heating, i.e., an increase of the excitation energy, results in a gradual destruction of the condensate and an increase in the

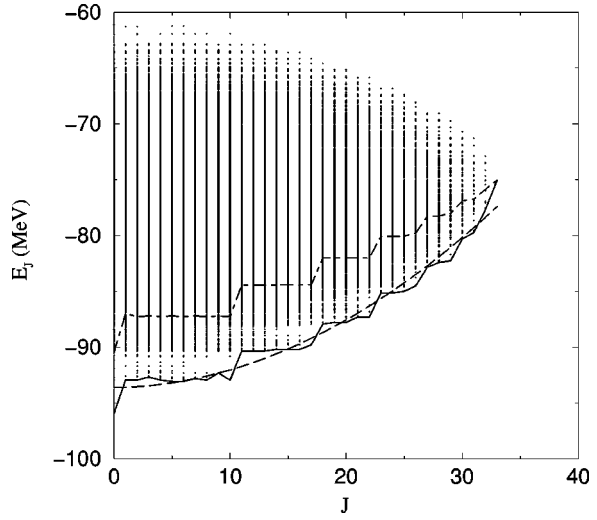

FIG. 13. Energies of all many-body states in ^{116}Sn vs their angular momentum; the yrast line (solid line) is fit by a parabola (dashed line), and the dashed-dotted curve corresponds to the yrast line in the degenerate case with all single-particle energies being equal.

normal component of the fluid (increase of seniority in nuclear physics terminology). Similarly, a higher angular momentum can be created only by a pair breaking. The unpaired particles can be coupled to a nonzero angular momentum which can be treated as some kind of rotation. When the spins allowed for a given seniority are fully aligned, any further increase of angular momentum requires a change of configuration and seniority jump, with the corresponding energy increase. This picture is qualitatively similar to the phenomenon of quantized vortex formation in superfluid liquid ^{4}He.

In Fig. 13 the energies of all eigenstates in ^{116}Sn within the shell model space (all possible seniorities) are marked by points in the energy versus angular momentum plane. The staircase yrast line, shown by a solid line in Fig. 13, is drawn through the states of maximum spin for each seniority. It can be fitted well by a parabola (dashed line), thus giving the average moment of inertia $I=32\ \mathrm{MeV}^{-1}$. This result can be compared with the classical moment of inertia of a rigid sphere with uniform density, $I_{\mathrm{rig}}=2MR^2/5$ with mass $M=938A$ MeV and radius $R=1.2A^{1/3}$ fm; for ^{116}Sn $I_{\mathrm{rig}}=35\ \mathrm{MeV}^{-1}$. It is known that in the adiabatic (linear response) approximation a cranked Fermi gas has a rigid body moment of inertia while pairing interactions usually reduce this value [1,2] by about a factor of 2. The above results show that the overall effect of pairing on the rotational properties is considerably quenched at high excitation energy. The broken pairs and pair vibrations return the moment of inertia to the original Fermi-gas value. This phenomenon has a direct analog in superfluid liquid ^{4}He, where a large number of vortices emerges at high rotation speed forming a lattice structure [35] which rotates as a whole restoring the rigid body moment of inertia and characteristic average velocity field.

Pairing vibrations are primarily responsible for mixing of states in paired systems, and therefore they are expected to have a profound effect on the properties of nuclear systems such as the high-spin moment of inertia. For calculating the yrast line shown on Fig. 13 as a dash-dotted line, we assume full degeneracy, making all ϵ_j is equal. This reduces the energy required for the pair transfer, and therefore makes pair vibrations stronger and more chaotic. As a result, the moment of inertia was even further increased to a value of $43\ \mathrm{MeV}^{-1}$. As can be expected in the degenerate model, where the perturbative cranking approach is not valid, the average angular momentum dependence on energy is vibrational (close to linear), and the quadratic contribution related to the inverse moment of inertia is small.

VIII. CONCLUSION

In this paper we discussed the properties of the pairing interaction in a finite quantum system described within the shell-model approach. This interaction, being a very important part of the general residual interaction, has specific features effective for pairs with total spin zero only. The standard approach takes into account the pairing effects with the aid of the BCS approximation borrowed from the theory of macroscopic superconductivity. This approximation fails not only from the viewpoint of particle number nonconservation which might be essential for finite systems, but also does not work for weak pairing and beyond the phase transition point. Therefore, we base our study on the earlier suggested exact numerical solution where the use of the quasispin symmetry provides necessary quantum numbers and simplifies the problem immensely.

The collective excitations in the paired system (pair vibrations) are traditionally described by developing the random-phase approximation on the background of the BCS ground state. We show that the exact solution differs from that in the BCS+RPA theory, especially in the region of the phase transition. This is seen clearly in the example of the realistic shell model for the ^{116}Sn nucleus as well as in the analytically solvable two-level model. Analogous results can be obtained for isospin-invariant pairing which will be considered elsewhere.

We have discussed the chaotic (incoherent) aspects of the pairing interaction. The residual interactions in general mix independent-particle configurations, creating complicated stationary many-body states. These effects influence both local and global statistical properties of the system. In the case of a generic residual interaction, we come locally to the GOE-like nearest level spacing distribution and enhanced spectral rigidity, whereas the global behavior reveals thermalization of the system. Typically, the interaction plays the role of a heat bath, bringing the single-particle occupancies close to the Fermi-Dirac distribution even in a strongly interacting system. The pairing interaction is in many respects exceptional. Although it induces the local level repulsion and increases information entropy of the eigenstates, the spectral rigidity shows a pseudo-oscillatory behavior related to the vibrational character of excitations. Both information (Shannon) and invariant (von Neumann) entropies distinctly reflect the existence of the phase transition. The normal behavior of the thermodynamic entropy associated with the level density

coexists with the absence of full thermalization of single-particle motion. The yrast line of the system reveals the trend to the rigid-body rotation at high excitation energy where many pairs are effectively broken.

Pure pairing cannot exist as the only two-body interaction (for a charged system it would violate the gauge invariance; also see Ref. [36]). As shown by the full analysis of the statistical properties of the nuclear shell model wave functions [3], the pairing can be considerably modified by the presence of other parts of the residual interaction. For example, the families of states corresponding to various values of the seniority quantum number are almost completely mixed although the pairing phase transition is still observed through the behavior of the pairing correlators for individual low-lying eigenstates [37]. However, beyond the phase transition there exists a long exponentially decreasing tail of dynamic pairing correlations. The interplay of pairing with other types of residual interaction is an interesting and promising problem for future research.

ACKNOWLEDGMENTS

We thank M. Hjorth-Jensen for providing the renormalized G matrix for the ^{132}Sn region. The work was supported by NSF Grant No. 0070911.

[1] S.T. Belyaev, Mat. Fys. Medd. Dan. Vid. Selsk. **31** (11) (1959); in *Selected Topics in Nuclear Theory*, edited by F. Janouch (IAEA, Vienna, 1963), p. 291.
[2] A. Bohr and B. Mottelson, *Nuclear Structure* (Benjamin, New York, 1974), Vol. 2.
[3] V. Zelevinsky, B.A. Brown, N. Frazier, and M. Horoi, Phys. Rep. **276**, 85 (1996).
[4] A. Volya, B.A. Brown, and V. Zelevinsky, Phys. Lett. B **509**, 37 (2001).
[5] A.K. Kerman, R.D. Lawson, and M.H. Macfarlane, Phys. Rev. **124**, 162 (1961).
[6] K.T. Hecht, Nucl. Phys. **63**, 177 (1965).
[7] K.T. Hecht, Phys. Rev. **139**, B794 (1965).
[8] A. Volya (unpublished).
[9] F. Andreozzi, L. Coraggio, A. Covello, A. Gargano, and A. Porrino, Z. Phys. A **345**, 253 (1996).
[10] N. Sandulescu, J. Blomqvist, T. Engeland, M. Hjorth-Jensen, A. Holt, R.J. Liotta, and E. Osnes, Phys. Rev. C **55**, 2708 (1997).
[11] R. Machleidt, F. Sammarruca, and Y. Song, Phys. Rev. C **53**, R1483 (1996).
[12] M. Hjorth-Jensen (private communication).
[13] M. Hjorth-Jensen, T.T.S. Kuo, and E. Osnes, Phys. Rep. **261**, 125 (1995); M. Hjorth-Jensen, H. Muther, E. Osnes, and A. Polls, J. Phys. G **22**, 321 (1996).
[14] A. Volya, B.A. Brown, and V. Zelevinsky, Prog. Theor. Phys. (to be published).
[15] A. Bohr, *International Symposium on Nuclear Structure* (Dubna, USSR, 1968) (International Atomic Energy Agency, Vienna, 1968), p. 179.
[16] D.R. Bès and R.A. Broglia, Nucl. Phys. **80**, 289 (1966).
[17] V. Zelevinsky, M. Horoi, and B.A. Brown, Phys. Lett. B **350**, 141 (1995).
[18] V. Sokolov, B.A. Brown, and V. Zelevinsky, Phys. Rev. E **58**, 56 (1998).
[19] F.J. Yonezawa, J. Non-Cryst. Solids **35&36**, 29 (1980).
[20] J. Reichl, Europhys. Lett. **6**, 669 (1988).
[21] F.M. Izrailev, Phys. Rep. **196**, 299 (1990).
[22] V.G. Zelevinsky, Nucl. Phys. **A555**, 109 (1993).
[23] V. Zelevinsky, Annu. Rev. Nucl. Part. Sci. **46**, 237 (1996).
[24] M. Horoi, B.A. Brown, and V. Zelevinsky, Phys. Rev. Lett. **87**, 062501 (2001).
[25] K.R.W. Jones, J. Phys. A **23**, L1247 (1990).
[26] P.W. Anderson, Phys. Rev. **112**, 1900 (1958).
[27] J. Bang and J. Krumlinde, Nucl. Phys. **A141**, 18 (1970).
[28] J.L. Woods, K. Heyde, W. Nazarevicz, M. Huyse, and P. Van Duppen, Phys. Rep. **215**, 101 (1992).
[29] D.G. Fleming, M. Blann, H.W. Fulbright, and J.A. Robbins, Nucl. Phys. **A157**, 1 (1970).
[30] D. Mulhall, A. Volya, and V. Zelevinsky, Phys. Rev. Lett. **85**, 4016 (2000).
[31] P. Cejnar, V. Zelevinsky, and V. Sokolov, Phys. Rev. E **63**, 036127 (2001).
[32] T.A. Brody, J. Flores, J.B. French, P.A. Mello, A. Pandey, and S.S.M. Wong, Rev. Mod. Phys. **53**, 385 (1981).
[33] M. Horoi, V. Zelevinsky, and B.A. Brown, Phys. Rev. Lett. **74**, 5194 (1995).
[34] I.C. Percival, J. Phys. B **6**, L229 (1973).
[35] C. Lane, *Superfluid Physics* (McGraw-Hill, New York, 1962).
[36] S.T. Belyaev, Yad. Phys. **4**, 936 (1966), [Sov. J. Nucl. Phys. **4**, 671 (1967)]; Phys. Lett. **28B**, 365 (1969).
[37] V. Zelevinsly, *Proceedings of the Conference on Nuclear Structure at the Limits* (Argonne National Laboratory, Argonne, 1997), p. 353.